


LA-8650-MS

LK. 2236

176  
1/27/81 T.S. 

①

MASTER

R-1442

**Finite Ion Larmor Radius Effects and  
Wall Effects on  $m = 1$  Instabilities**

University of California



**LOS ALAMOS SCIENTIFIC LABORATORY**

Post Office Box 1663 Los Alamos, New Mexico 87545

# Finite Ion Larmor Radius Effects and Wall Effects on $m = 1$ Instabilities

Thomas E. Cayton

**DISCLAIMER**

This document contains preliminary data. It is subject to change without notice. It is not to be distributed outside the laboratory. It is not to be used for advertising or promotional purposes, for creating new products, or for resale.



FINITE ION LARMOR RADIUS EFFECTS AND  
WALL EFFECTS ON  $m = 1$  INSTABILITIES

by

Thomas E. Cayton

ABSTRACT

A set of fluid-like equations that simultaneously includes effects due to geometry and finite ion gyroradii is used to examine the stability of a straight, radially diffuse screw pinch in the regime where the poloidal magnetic field is very small compared with the axial magnetic field. It is shown that this pinch may be rendered completely stable through a combination of finite Larmor radius effects and wall effects. Many of the  $m = 1$  modes of the diffuse pinch can be stabilized by finite ion Larmor radius effects, just as all flute modes can be stabilized. Because of the special nature of the  $m = 1$  eigenfunctions, finite ion gyroradius effects are negligible for the kink modes of very large wavelength. This special nature of the eigenfunctions, however, makes these modes good candidates for wall stabilization. The finite Larmor radius stabilization of  $m = 1$  modes of a diffuse pinch is contrary to the conventional wisdom that has evolved from studies of sharp-boundary, skin-current models of the pinch.

---

I. INTRODUCTION

In a recent article, Pearlstein and Freidberg<sup>1</sup> derived a set of linearized fluid-like equations suitable for investigating the stability of hot-ion, high- $\beta$ , near  $\theta$ -pinch configurations to low-frequency, long-wavelength perturbations. These fluid-like equations were extracted by asymptotic expansion from a version of the Vlasov-fluid model<sup>2</sup> that includes finite electron pressure<sup>3,4</sup> under the assumptions that the ion gyroradius is very small compared with the pinch radius, and simultaneously, that the non-axial magnetic field components that drive instabilities in ideal magnetohydrodynamics are very small compared with the axial magnetic field.

(By "very small" we mean sufficiently small that only the leading-order terms in the asymptotic series expansions need to be retained.) The system of equations that results from this finite Larmor radius ordering include effects due to geometry, as does ideal magnetohydrodynamics; but, it also includes effects due to the kinetic ions, particularly, the electric and gradient-B drifts. To the order that the calculation has been carried, certain other ion kinetic effects cancel exactly and, therefore, are not represented in the finite Larmor radius equations; examples of effects which cancel exactly include: resonant particles, drifts due to the non-axial magnetic field components, and inertial drifts. In this report we apply this finite Larmor radius description of Ref. 1 to study the effects of finite ion gyroradii on magnetohydrodynamic instabilities of straight, cylindrically symmetric, radially diffuse screw pinch equilibria.

In previous related work, Wright, et al.<sup>5</sup> expanded the Vlasov equation in a finite Larmor radius limit to obtain a dispersion differential equation governing the modes of cylindrically symmetric, radially diffuse configurations. In general, the model developed in Ref. 5 admits a broader class of distribution functions than that of Ref. 1; however, Ref. 5 considers only cylindrically symmetric pinches, whereas Ref. 1 allows arbitrary geometry for configurations dominated by an axial magnetic field. In the absence of equilibrium pressure anisotropy, flow, and heat flux the differential equations derived and studied in Ref. 5 are entirely equivalent to the ones studied here. Furthermore, many of the results reported here are also mentioned in Ref. 5.

Finite ion gyroradius effects on the stability of the sharp-boundary, skin-current model of the screw pinch have been studied and delineated by several authors.<sup>1,6-9</sup> For the sharp-boundary pinch both analytical<sup>1,8-9</sup> and numerical<sup>6-7</sup> results demonstrate that flute modes with azimuthal mode number  $m > 2$  are stabilized by finite ion gyroradius effects, but that kink modes with  $m = 1$  behave quite differently and are not stabilized. In fact, the growth rates of  $m = 1$  instabilities in the Vlasov-fluid description of the sharp-boundary pinch are precisely the same as the ones predicted by ideal magnetohydrodynamics. Thus, a conventional wisdom concerning finite gyroradius stabilization has evolved, namely, that  $m = 1$  modes are unaffected.

Wright, et al.<sup>5</sup> describe the modifications of Suydam modes by finite ion Larmor radius effects in a radially diffuse screw pinch. A marked lack of influence of gyroradius effects on  $m = 1$  modes in comparison with higher  $m$  instabilities is noted. However, data presented in Ref. 5 indicate that  $m = 1$  modes are affected to some degree by finite ion gyroradii. Thus, results obtained with diffuse radial profiles disagree with those of the sharp-boundary model that predict  $m = 1$  modes to be completely free of finite ion gyroradius effects.

In this report we examine, both numerically and analytically, the linear stability of radially diffuse screw pinch equilibria. Our results demonstrate that combinations of finite Larmor radius stabilization and wall stabilization can eliminate all magnetohydrodynamic instabilities, including  $m = 1$  modes; a stability criterion involving the ion gyroradius and the wall radius is presented. We find that some of the  $m = 1$  modes can be finite Larmor radius stabilized, contrary to the conventional wisdom; this is a consequence of the diffuse equilibrium profiles. On the other hand, we find that ion gyroradius effects are negligible for very long wavelength  $m = 1$  modes; again, this is a consequence of the detailed radial structure of the  $m = 1$  eigenfunctions and the diffuse equilibrium profiles. The finite Larmor radius contribution to the eigenvalue problem for  $m = 1$  modes is shown to consist of an overlap-type integral involving the equilibrium magnetic field gradient and the squared magnitude of the gradient of the radial eigenfunction. An approximate, algebraic equation for the eigenfrequencies of  $m = 1$  modes is developed by using, for the eigenfunction, a trial function that is suggested by the numerical results. This algebraic approximation illuminates the behavior of the  $m = 1$  mode, and the necessity for both finite Larmor radius stabilization and wall stabilization to achieve a completely stable pinch.

The report is organized as follows. In Sec. II, the model is introduced, notation is established, and the finite Larmor radius equations that govern the perturbations of the equilibria are stated. Numerical results are presented in Sec. III. We show that some of the  $m = 1$  modes are finite Larmor radius stabilized, just as are all  $m > 2$  modes. The parameter boundary for a completely stable pinch is explored. In Sec. IV, we cast the eigenvalue problem in variational form and derive, using trial functions, an approximate quadratic equation for the eigenfrequencies. Section V consists of a summary and conclusions.

## II. THE MODEL

We shall use the fluid-like equations of Ref. 1 to investigate the effect of finite ion gyroradii upon the unstable magnetohydrodynamic modes of straight, cylindrically symmetric screw pinch equilibria. The equations that govern the equilibrium and perturbation quantities are obtained from the leading-order terms of appropriate asymptotic expansions. The derivation begins with the Vlasov-fluid model<sup>2</sup> of the pinch. In cylindrical polar coordinates, the equilibrium density,  $\rho$ , pressure,  $p$ , and the magnetic field components,  $B_\theta$  and  $B_z$ , are functions only of the radial coordinate,  $r$ , and satisfy the equations of ideal magneto-hydrostatics.<sup>1,2</sup> However, to utilize the results of Ref. 1, we must restrict our attention to near  $\theta$ -pinch equilibria, where

$$B_\theta \ll B_z . \quad (1)$$

Also, we assume that the gyroradius of a typical ion,  $r_L$ , is small compared with the radius of the pinch,  $a$ . These two assumptions guarantee that both the growth rates of magnetohydrodynamic instabilities and the characteristic ion drift frequencies (i.e., the electric and gradient-B drifts) are small compared with the characteristic magnetohydrodynamic frequency [the inverse transit-time of an Alfvén wave across the column,  $B_z/(\rho^{1/2}a)$ ]. Although the growth rate and the drift frequencies are all small quantities, the magnitudes are themselves comparable, so that geometric and ion kinetic effects are handled on the same basis. This is the basic finite Larmor radius ordering.

We use a system of units whose characteristic length, mass, and time are defined in terms of the following physical quantities: 1) the equivalent sharp-boundary radius of the pinch,  $a$ ; 2) the mass density measured on the axis of the pinch,  $\rho_0$ ; 3) the magnetic field measured far from the pinch,  $B_{z\infty}$ . To give precise meaning to the adjective "small", we introduce a smallness parameter  $\mu$ ,

$$\mu \equiv B_\theta(r/a=1)/B_{z\infty} ,$$

and we scale the equilibrium quantities as follows (scaled quantities are denoted by a tilde):

$$B_{\theta} = \mu \tilde{B}_{\theta},$$

$$B_z = \tilde{B}_z,$$

$$\rho = \hat{\rho},$$

$$p = \hat{p}.$$

To leading order, the equilibrium pressure and magnetic field components satisfy the  $\theta$ -pinch pressure balance relation,

$$\hat{p} + \frac{1}{2} \tilde{B}_z^2 = \frac{1}{2}, \quad (2)$$

where  $B_{\theta}$  is, to leading order, an arbitrary function of  $r$ . Numerical results presented in Sec. III are obtained using the rigid-rotor profiles of Ref. 10,

$$\rho(r) = \rho_0 \frac{\operatorname{sech}^2(r^2/r_0^2 + \alpha)}{\operatorname{sech}^2 \alpha}, \quad (3)$$

$$B_z(r) = B_{z\infty} \tanh(r^2/r_0^2 + \alpha), \quad (4)$$

$$B_{\theta}(r) = \mu B_{z\infty} \left( \frac{r_0}{r} \right) \frac{\tanh(r^2/r_0^2 + \alpha) - \tanh \alpha}{1 - \tanh \alpha}, \quad (5)$$

where the parameter  $\alpha$  is related to the plasma  $\beta$  by  $\beta = \operatorname{sech}^2 \alpha$ , and  $r_0 = [1 + (1 - \beta)^{1/2}]^{1/2} a$ . We assume that the temperature is uniform and, hence that the pressure is proportional to density,

$$\hat{p}(r) = \frac{\beta}{2} \hat{\rho}(r) . \quad (6)$$

Equations (3)-(6) specify the equilibrium in terms of the expansion parameter  $\mu$  and a single parameter  $\beta$ ; Eq. (1) is satisfied by virtue of the scaling and the expansion parameter  $\mu$  that appears in Eq. (5). The plasma is assumed to extend to a rigid perfectly conducting cylindrical surface at  $r = b$ . Therefore, the configuration is characterized by two dimensionless parameters,  $\beta$  and  $b/a$ , in addition to the expansion parameter  $\mu$ .

The linear stability problem is formulated in terms of a vector  $\xi_1$ , the displacement of the electron fluid. Because of the symmetry of the equilibrium, we assume that all perturbation quantities are of the form

$$r(r, \theta, z, t) = r(r) \exp[i(m\theta + kz - \omega t)] ,$$

where  $m$ ,  $k$ , and  $\omega$  are parameters. The finite Larmor radius description of Ref. 1 applies to long-wavelength, low-frequency perturbations. To satisfy these criteria we introduce the following scaled quantities:

$$\omega = \mu \tilde{\omega} ,$$

$$k = \mu \tilde{k} ,$$

$$r_L/a = \mu \tilde{r}_L/a .$$

$r_L$  is the thermal gyroradius of a typical ion.

Now Pearlstein and Freidberg<sup>1</sup> have shown that, to lowest order, the radial component of the displacement,  $\xi_r$ , satisfies a single second-order ordinary differential equation [Eq. (40) of Ref. 1]. In the notation used here, the equation reads (the tilde is suppressed hereafter):

$$\left[ \Lambda_{fr}(r\xi_r) \right]' - \frac{m^2}{r} \Lambda_{fr}\xi_r + \omega\sigma r\xi_r + 2m \left[ \left( \frac{b_\theta}{r} \right) k B_z + \left( \frac{B_\theta}{r} \right) F \right] r\xi_r = 0 , \quad (7)$$



where a prime denotes differentiation with respect to  $r$ ,

$$\Delta_f = \rho \omega' - \omega \rho - F^2 ,$$

$$F = k E_z + \frac{m}{r} B_z' ,$$

and

$$\sigma = \beta^{-1/2} \frac{m}{2} \frac{r_L}{a} \left\{ \frac{1}{r} \left( 1 + \frac{1}{B_z^2} \right) B_z' \right\} .$$

The solution of Eq. (7) subject to the boundary conditions

$$(r \xi_r) |_{r=0} = 0 , \quad (8)$$

and

$$(r \xi_r) |_{r=b} = 0 , \quad (9)$$

determines the complex eigenvalue  $\omega$  and eigenfunction  $\xi_r$ . In the limit that the ion gyroradius vanishes, the parameter  $r_L/a$ , the scaled Larmor radius divided by the plasma radius, equals zero and the eigenvalue problem, Eqs. (7)-(9), is precisely the same as the one derived from leading order ideal magnetohydrodynamics<sup>11</sup> or the leading order guiding center plasma description.<sup>12</sup> In the next section we use Eqs. (7)-(9) to study the effects of finite ion gyroradii upon magnetohydrodynamic instabilities. Note that the parameter  $r_L/a$  occurs in the combination  $\beta^{-1/2} m r_L/2a$ , therefore, the influence of finite ion gyroradii increases with increasing azimuthal mode number  $m$ , and with decreasing  $\beta$ .

### III. NUMERICAL RESULTS

In this section we present specific results obtained by numerical solution of Eqs. (7)-(9). These computations were executed using the equilibrium profiles specified in Eqs. (2)-(6). Figures 1-3 show the dependence upon scaled axial wavevector,  $(ka/\mu)$ , of the scaled growth rate,  $(\omega_i a/\mu v_A)$ , for  $m = 3$ ,  $m = 2$ , and  $m = 1$  modes, respectively, when  $\beta = 0.75$ , and  $(b/a) = 5.0$ , for several values of the Larmor radius parameter,  $(r_L/\mu a)$ .  $v_A$  is a characteristic value of the Alfvén speed defined by  $v_A^2 \equiv B_{z0}^2/\mu_0$ . When  $(r_L/\mu a) = 0$ , the solution is identical to that in ideal magnetohydrodynamics (and isotropic guiding center plasma theory). Figures 1 and 2 illustrate the influence of finite ion Larmor radius effects upon  $m \neq 1$  modes. All unstable ideal magnetohydrodynamic modes are stabilized when  $(r_L/\mu a)$  assumes rather modest values. Note that finite ion Larmor radius effects are more pronounced for the modes with a larger azimuthal mode number,  $m$ : As mentioned in Sec. II, the relevant quantity is  $m \times (r_L/\mu a)$ . The same qualitative features are exhibited by modes with  $m > 3$ . Thus, ideal magnetohydrodynamic modes with  $m > 1$  can easily be stabilized by finite ion Larmor radius effects.

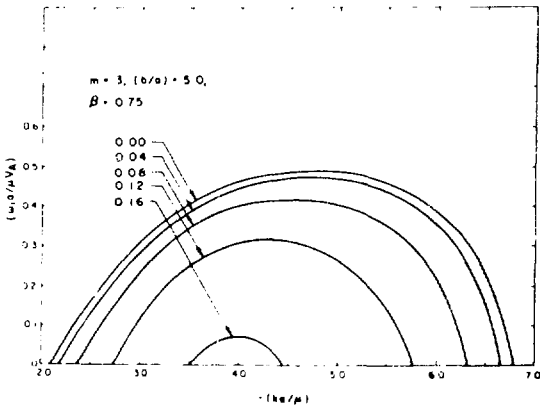


Fig. 1. Scaled growth rate for  $m = 3$  modes versus scaled axial wavenumbers for several values of  $(r_L/\mu a)$ . The pinch is stable to  $m = 3$  perturbations when  $(r_L/\mu a) \geq 0.18$ .

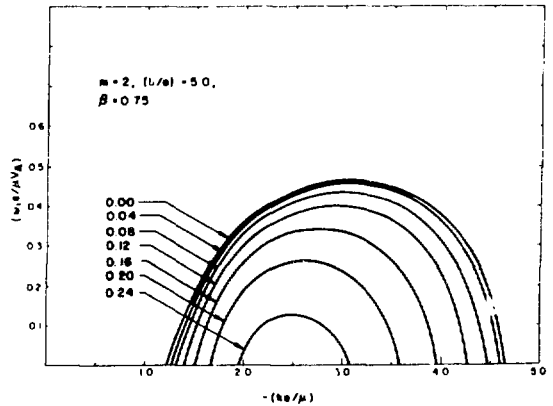


Fig. 2. Scaled growth rate for  $m = 2$  modes versus scaled axial wavenumbers for several values of  $(r_L/\mu a)$ . The pinch is stable to  $m = 2$  perturbations when  $(r_L/\mu a) \geq 0.28$ .

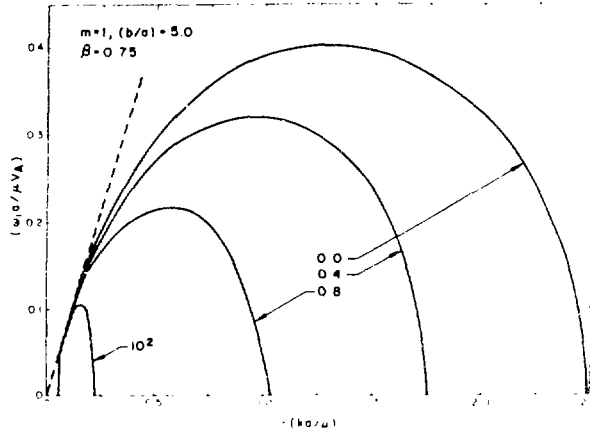


Figure 3.

Scaled growth rate for  $m = 1$  modes versus scaled axial wavenumber for several values of  $(r_L/a)$ . Long-wavelength instabilities are not affected by finite ion Larmor radius effects, even for extremely large values of  $(r_L/a)$ . The dashed line is a plot of Eq. (20). Wall effects eliminate the modes with  $-(ka/a) < 0.07$ .

Figure 3 illustrates the influence of finite ion Larmor radius effects upon  $m = 1$  modes, for the same equilibrium configuration used for Figs. 1 and 2. In this case, the required values of  $(r_L/a)$  are much larger than in Fig. 2 and some unstable ideal magnetohydrodynamic modes remain unaffected by even very large values of the parameter. Thus, while some of the  $m = 1$  modes can be finite Larmor radius stabilized, other ones, those of long axial wavelength, cannot. The dashed line in Fig. 3 shows the growth rate for the "internal kink" or "interchange" mode<sup>13</sup> when the plasma region includes all space:  $\omega_1 = \frac{1}{2} k$ . These modes have a singular (mode rational) surface (denoted by  $r = r_s$ ) that recedes to infinity,  $r_s \rightarrow \infty$ , as  $k \rightarrow 0$ . The eigentunctions of these instabilities cause uniform translation of all plasma within the singular surface. When the plasma region is bounded by a rigid perfectly conducting cylindrical surface at  $r = b$ , only modes whose singular surface lies within the conducting shell,  $r_s < b$ , can exist. This is a manifestation of wall stabilization. In Fig. 3 wall effects stabilize modes whose axial wavenumber is sufficiently small,  $-(ka/a) < 0.07$ .

In Fig. 4, the perfectly conducting wall has been moved from  $(b/a) = 5.0$  to  $(b/a) = 2.0$ , while all the other parameters are the same as in Fig. 3. Wall effects now eliminate all unstable modes with  $-(ka/a) < 0.2$ ; the

remaining unstable ideal magnetohydrodynamic modes may be finite ion Larmor radius stabilized. Thus, an appropriate combination of wall effects and finite ion Larmor radius effects can render the pinch completely stable to ideal magnetohydrodynamic modes;  $m = 1$  modes are the most tenacious, however.

To illuminate the nature of the  $m = 1$  mode, we plot in Fig. 5 the radial eigenfunction of a typical mode; the equilibrium density profile is also plotted. Note that the gradient of the eigenfunction is negligible except in the vicinity of the singular surface,  $r = r_s$ , where it is large. On the other hand, the gradients of the leading-order equilibrium quantities,  $\rho'$ ,  $p'$ , and  $B_z'$ , all become vanishingly small as  $r$  increases. Since the finite Larmor radius contribution in Eq. (7),  $\sigma$ , is directly proportional to  $B_z'$ , finite ion Larmor radius effects are negligible for  $m = 1$  modes whose singular surfaces occur at large values of  $r$ .

We further examine the  $m = 1$  eigenfunctions in Fig. 6 where we plot (with a dashed line) the radius of the singular surface,  $r_s$ , against the scaled axial wavevector,  $(ka/\mu)$ ; the Suydam radius,  $r_{\text{SUYDAM}}$ , inside of which the Suydam criterion is violated [i. e.,  $p' + rB_z^2(v'/v)^2/8 < 0$ , where  $v = B_z/rB_z$ ] is shown with a broken line. Finally, we plot (with a solid line) the

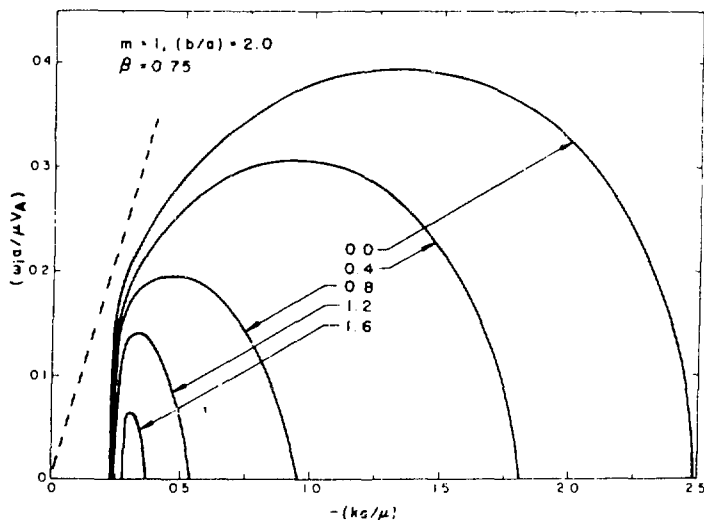


Figure 4.

Scaled growth rate for  $m = 1$  modes versus scaled axial wavenumber for several values of  $(r_L/\mu a)$ . The compression ratio has been reduced from  $(b/a) = 5.0$  in Fig. 3 to  $(b/a) = 2.0$  in this case. Wall effects now eliminate modes with  $-(ka/\mu) < 0.2$ . The pinch is stable to  $m = 1$  perturbations when  $(r_L/\mu) > 1.7$ .

position where the radial eigenfunction of the unstable  $m = 1$  mode assumes the value 0.5, denoting this by  $r_{1/2}$ , against the scaled axial wavenumber,  $(ka/\mu)$ . From Fig. 6 we can see that the equilibrium configuration is actually unstable for a wider range of  $(ka/\mu)$  than is predicted by the Suydam criterion; this result has been reported previously by Freidberg.<sup>10</sup> Note that the half-radii of the  $m = 1$  modes,  $r_{1/2}$ , and the radii of the singular surfaces,  $r_s$ , agree very well, particularly for small values of  $(ka/\mu)$ , except near the conducting wall. We shall make use of this feature of  $m = 1$  modes in Sec. IV.

Because of the special nature of the  $m = 1$  eigenfunction, a combination of wall effects and finite ion Larmor radius effects is required to achieve a completely stable pinch. The stability boundary is plotted in Fig. 7 as a function of the wall radius,  $(b/a)$ , and the critical value of the Larmor radius parameter,  $N = (r_L/\mu a)_c$ , for three values of  $\beta$ . As mentioned in Sec. II, finite Larmor radius stabilization is more effective in

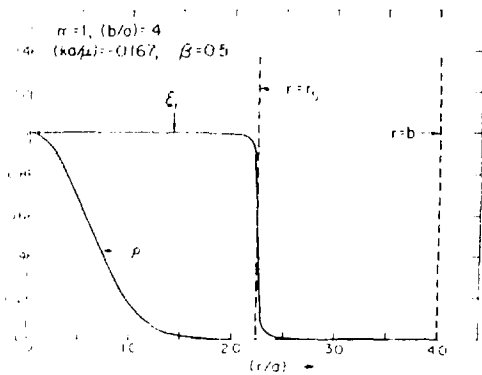


Fig. 5. The radial eigenfunction of a typical long-wavelength  $m = 1$  instability. The equilibrium density profile is also shown.

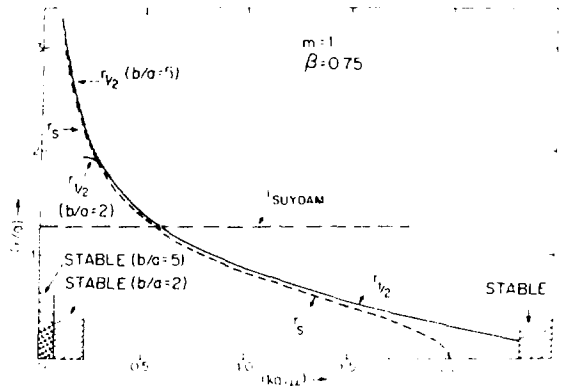


Fig. 6. Dependence on the scaled axial wavenumber of the half radius of the  $m = 1$  eigenfunction,  $r_{1/2}$ , and of the radii of the singular surface,  $r_s$  (dashed line). This Suydam criterion is violated when the curve  $r = r_s$  lies below the broken line  $r = r_{\text{SUYDAM}}$ . However, the pinch is unstable to a larger range of axial wavenumbers than the Suydam criterion indicates.

configurations with smaller  $\beta$ . Note that  $N$ , the required value of  $r_L/\rho a$ , increases rapidly as the conducting wall radius increases. This is a consequence of the long-wavelength  $m = 1$  instabilities; the same effect is illustrated in Figs. 3 and 4.

Finally, we use the results of Fig. 7 to determine the maximum axial current permitted for a pinch to be stable to all ideal magnetohydrodynamic modes, including  $m = 1$  modes. Unraveling the scaling and changes of variable that have occurred, we find

$$I[\text{kA}] < \frac{32.3}{N(b/a)} (T[\text{keV}])^{1/2}, \quad (10)$$

where brackets denote the dimensions of the current and temperature of the plasma and  $N(b/a)$  is the function that determines the boundary curve in Fig. 7. For example, for a near  $\zeta$ -pinch configuration having the parameters  $T = 1\text{keV}$ ,  $\beta = 0.75$ , and  $(b/a) = 2.2$  the maximum axial current permitted by magnetohydrodynamic stability considerations is  $I \approx 16\text{kA}$ ; if the compression ratio is increased to  $(b/a) = 2.8$ , the maximum permissible axial current is

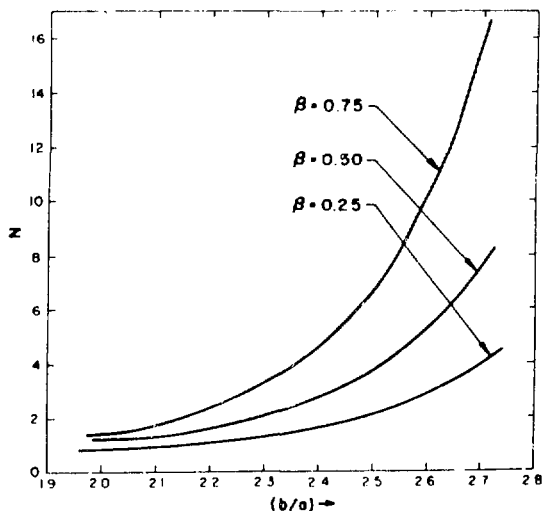


Figure 7.

Stability boundary for the diffuse screw pinch, for three values of  $\beta$ . The area above the curve corresponds to stability to all ideal magnetohydrodynamic modes.

$\Gamma = 2kA$ . These examples emphasize the important role played by wall effects in overcoming long-wavelength  $m = 1$  modes.

#### IV. VARIATIONAL FORMULATION

By multiplying Eq. (7) by  $r \frac{r^*}{r}$  (an asterick denotes complex conjugation) and integrating over the interval  $0 \leq r \leq b$ , we cast Eq. (7) in the form

$$\omega^2 A + \omega B + C = 0 \quad , \quad (11)$$

where

$$A = \int_0^b \left[ r^2 |r'_r|^2 + (m^2 - 1) |r_r|^2 \right] r dr$$

$$- \int_0^b r^2 |r_r|^2 r^2 dr \quad , \quad (12)$$

$$B = - \epsilon^{-1/2} \frac{\bar{m}}{2} \frac{r_L}{a} \int_0^b \left( 1 + \frac{1}{B_z^2} \right) B_z^2 \left[ r^2 |r'_r|^2 + (m^2 - 1) |r_r|^2 \right] dr \quad , \quad (13)$$

$$C = - \int_0^b F'' \left[ r^2 |r'_r|^2 + (m^2 - 1) |r_r|^2 \right] r dr$$

$$- \beta k' \int_0^b r^2 |r_r|^2 r^2 dr \quad . \quad (14)$$

Because the coefficients A, B, and C in Eq. (11) depend on  $\omega$  implicitly the dispersion equation is more complicated than a quadratic equation. Furthermore, no minimum principle exists for this problem, which involves complex eigenvalues; the usual variational method that is employed in quantum mechanics to estimate eigenvalues does not apply. Nevertheless, some qualitative features can be extracted through the use of trial functions approximating the eigenfunction.

For  $m = 1$  modes, Eqs. (12)-(14) become

$$A = \int_0^b \rho |\xi_r^<|^2 r^3 dr - \int_0^b \rho' |\xi_r^<|^2 r^2 dr \quad , \quad (15)$$

$$B = -\frac{\beta^{-1/2} r_L}{2} \frac{r_L}{a} \int_0^b \left(1 + \frac{1}{B_z^2}\right) B_z^2 |\xi_r^<|^2 r^2 dr \quad , \quad (16)$$

$$C = -\int_0^b R^2 |\xi_r^<|^2 r^3 dr - \beta k^2 \int_0^b \rho' |\xi_r^<|^2 r^2 dr \quad . \quad (17)$$

Equation (11) reduces to the ideal magnetohydrodynamic result when the coefficient  $B$  vanishes. Therefore,  $m = 1$  instabilities can only be influenced by finite ion Larmor radius effects when a nonvanishing overlap exists between the gradient of the eigenfunction,  $\xi_r^<$ , and the gradient of the leading-order equilibrium magnetic field,  $B_z^2$ . This is negligibly small for long-wavelength  $m = 1$  instabilities whose singular surfaces occur at large values of  $r$ , where the gradients of the equilibrium quantities are negligible.

Now, consider the following trial function for long-wavelength  $m = 1$  modes, as suggested in Fig. 5

$$\begin{aligned} & 1 \quad , \quad r < r_h - \epsilon \\ \xi_r^< & = \frac{r_h + \epsilon - r}{2\epsilon} \quad , \quad r_h - \epsilon < r < r_h + \epsilon \\ & 0 \quad , \quad r_h + \epsilon < r \end{aligned} \quad (18)$$

where  $r_h$  and  $\epsilon$  are parameters, which specify the half radius and gradient thickness of the eigenfunction, respectively. For small values of  $\epsilon$ , the



gradient of this trial function vanishes except in the vicinity of the point  $r = r_{\text{H}}$ ,

$$\begin{aligned} 0 &, & r < r_{\text{H}} - \\ \frac{d\psi}{dr} &= -\frac{1}{2} & r_{\text{H}} - \epsilon < r < r_{\text{H}} + \epsilon \\ 0 &, & r_{\text{H}} + \epsilon < r \end{aligned} \quad (18)$$

Substituting Eqs. (18) and (19) into Eqs. (15)-(17) and expanding, we obtain the following,

$$A = -\frac{(r_{\text{H}} - r_{\text{H}})^2}{2} + 2 \int_{r_{\text{H}} - \epsilon}^{r_{\text{H}} + \epsilon} r dr - (r_{\text{H}} - r_{\text{H}})^2 + (0) \quad ,$$

$$B = -\frac{r_{\text{H}}^2 - r_{\text{H}}^2}{2} - \frac{r_{\text{H}}}{a} \left(1 + \frac{1}{B_Z}\right) B_Z^2 \Big|_{r=r_{\text{H}}} + (0) \quad ,$$

$$C = -\frac{(r_{\text{H}} - r_{\text{H}})^2}{2} - \frac{F(r_{\text{H}}) - F(r_{\text{H}})}{2} + ik^2 \int_{r_{\text{H}} - \epsilon}^{r_{\text{H}} + \epsilon} r dr - (r_{\text{H}} - r_{\text{H}})^2 + (0) \quad ,$$

where  $r_{\text{S}}$  denotes the radius of the singular surface,  $F(r_{\text{S}}) = 0$ . The singular surfaces for long-wavelength instabilities occur at large  $r_{\text{H}}$ ; furthermore, Fig. 5 shows that  $r_{\text{H}} \approx r_{\text{S}}$ . Therefore, an approximate dispersion equation for long-wavelength  $m = 1$  modes is

$$\omega^2 + \beta k^2 = 0 \quad ,$$

and the growth rate for this instability is

$$\gamma_i = \frac{1}{2} \omega_i R. \quad (20)$$

As  $k$  is increased, the solution of Eq. (11) deviates from the linear relationship between  $\omega_i$  and  $k$ , due to field line bending (which decreases  $\omega_i$ ) and inertia (which increases  $\omega_i$ ). Finite ion Larmor radius effects are negligible for this type of instability. These features are illustrated in Figs. (8) and (9), where the imaginary and real parts of the complex eigenvalue are plotted against  $k$ .

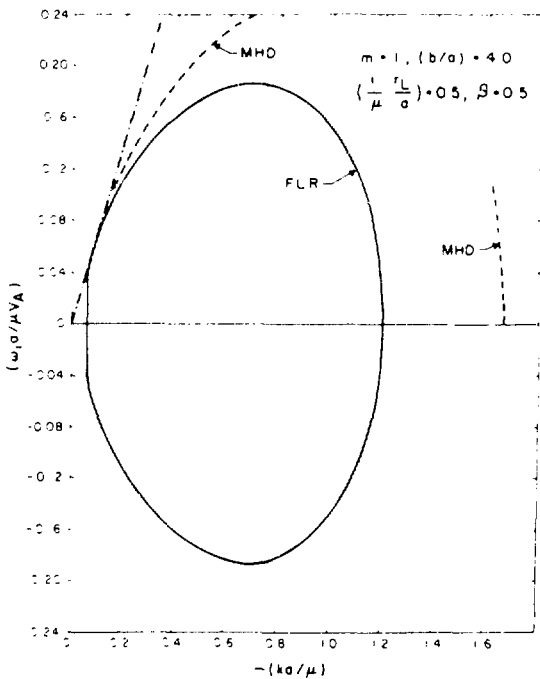


Fig. 8. Imaginary part of the complex frequency versus axial wavenumber. The eigenvalues of Eq. (11) occur as complex conjugate pairs when  $-(ka/\mu) < 1.2$ , and as two purely real solutions when  $-(ka/\mu) > 1.2$ .

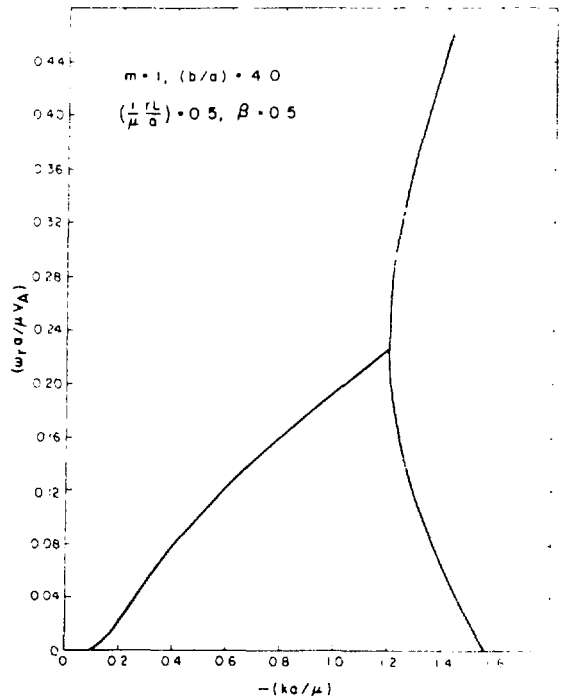


Fig. 9. Real part of the complex frequency versus axial wavenumber. The eigenvalues of Eq. (11) occur as complex conjugate pairs when  $-(ka/\mu) < 1.2$ , and as two purely real solutions when  $-(ka/\mu) > 1.2$ .

## V. DISCUSSION

We have examined the stability of a strand of finite length  $L$  in a flow plane. In the analysis, we neglected the magnetic field  $B_z$  (i.e., small compared with the axial field). It has been shown that this pinch can be rendered completely stable through an combination of a finite axial magnetic field and wall currents. The stability analysis is more involved than that of a finite length or radius current. In addition, we have identified the critical radius  $a_c$  for stability for finite length or radius current. The results show that for the diffuse equilibrium profiles,  $a_c$  is less than that of the conventional pinch that is confined to the center of the sharp boundary, which is not the case for the plane flow case. In addition, for a finite length current, the stability for long-wavelength modes is a function of the axial magnetic field. In particular, a strong axial magnetic field is required to stabilize the long-wavelength modes. The stability analysis of the special case of a finite length current is well established and is completely stable for a finite length  $L$  in the  $x$ -direction (i.e.,  $L > 0$ ).

## ACKNOWLEDGMENT

This investigation was supported by the program with the Department of Energy integrated research program. The author is grateful to Dr. J. Freidberg for his constructive comments. This work was supported by the program with the Department of Energy.

## REFERENCES

1. M. A. Helliwell and R. W. Longmire, "Magnetically confined plasma in the presence of a uniform axial field," *Phys. Fluids*, **1**, 114 (1958).
2. G. L. Friedberg, "The  $\alpha$ -Pinch," *Phys. Fluids*, **1**, 114 (1958).
3. R. Darwin, "The  $\alpha$ -Pinch Model with a finite length," *Phys. Fluids*, **1**, 114 (1958). Laboratory report #4618-MS, 1958.
4. T. R. Davidson, "Energy Analysis of the  $\alpha$ -Pinch Model," *Phys. Fluids*, **1**, 114 (1958).
5. R. L. Mittleman, D. L. S. Post, and M. G. Reines, "Stability considerations of a finite length  $\alpha$ -Pinch," *Phys. Fluids*, **15**, 114 (1972).

6. H. R. Lewis and J. P. Freilich, "Application of the Maslov-Platz Model to Helix-Belt Stability," in *Vibration Engineering: Conference on Control, Design and Physical Design of Structures*, The Centre for Research in Dynamics, Grenoble, France, 1984, pp. 1-11. (See also H. R. Lewis and J. Turner, "Stability Analysis of Turbine-Generator-Mass-Elipsoid-Rewind-Equilibrium," *Pulsed High Rate Events*, 1984, pp. 1-10, 1985, pp. 1-10, 1986, pp. 1-10.)
7. H. R. Lewis and J. Turner, "Finite-Element Analysis of Helix-Belt Stability in Turbines with Turbine-Generator-Mass-Elipsoid-Rewind," *ASME JOURNAL OF VIBRATION AND ACOUSTICS*, 1987, pp. 1-10.
8. J. Turner, "Finite-Element Analysis of Helix-Belt Stability in Turbine-Generator-Mass-Elipsoid-Rewind," *ASME JOURNAL OF VIBRATION AND ACOUSTICS*, 1987, pp. 1-10.
9. J. Turner, "Finite-Element Analysis of Helix-Belt Stability in Turbine-Generator-Mass-Elipsoid-Rewind," *ASME JOURNAL OF VIBRATION AND ACOUSTICS*, 1987, pp. 1-10.
10. J. Turner, "Finite-Element Analysis of Helix-Belt Stability in Turbine-Generator-Mass-Elipsoid-Rewind," *ASME JOURNAL OF VIBRATION AND ACOUSTICS*, 1987, pp. 1-10.
11. J. Turner, "Finite-Element Analysis of Helix-Belt Stability in Turbine-Generator-Mass-Elipsoid-Rewind," *ASME JOURNAL OF VIBRATION AND ACOUSTICS*, 1987, pp. 1-10.
12. J. Turner, "Finite-Element Analysis of Helix-Belt Stability in Turbine-Generator-Mass-Elipsoid-Rewind," *ASME JOURNAL OF VIBRATION AND ACOUSTICS*, 1987, pp. 1-10.
13. J. Turner, "Finite-Element Analysis of Helix-Belt Stability in Turbine-Generator-Mass-Elipsoid-Rewind," *ASME JOURNAL OF VIBRATION AND ACOUSTICS*, 1987, pp. 1-10.
14. J. Turner, "Finite-Element Analysis of Helix-Belt Stability in Turbine-Generator-Mass-Elipsoid-Rewind," *ASME JOURNAL OF VIBRATION AND ACOUSTICS*, 1987, pp. 1-10.
15. J. Turner, "Finite-Element Analysis of Helix-Belt Stability in Turbine-Generator-Mass-Elipsoid-Rewind," *ASME JOURNAL OF VIBRATION AND ACOUSTICS*, 1987, pp. 1-10.